



OPEN ACCESS

EDITED BY
Erika Kague,
University of Bristol, United Kingdom

REVIEWED BY
Ann Huysseune,
Ghent University, Belgium
James Nichols,
University of Colorado, United States
J. Gage Crump,
University of Southern California,
United States

*CORRESPONDENCE
Pierre Le Pabic
lepabicp@uncw.edu
Thomas F. Schilling
tschilli@uci.edu

SPECIALTY SECTION
This article was submitted to
Bone Research,
a section of the journal
Frontiers in Endocrinology

RECEIVED 02 October 2022
ACCEPTED 17 November 2022
PUBLISHED 06 December 2022

CITATION
Le Pabic P, Dranow DB, Hoyle DJ
and Schilling TF (2022) Zebrafish
endochondral growth zones
as they relate to human bone size,
shape and disease.
Front. Endocrinol. 13:1060187.
doi: 10.3389/fendo.2022.1060187

COPYRIGHT
© 2022 Le Pabic, Dranow, Hoyle and
Schilling. This is an open-access article
distributed under the terms of the
[Creative Commons Attribution License
\(CC BY\)](https://creativecommons.org/licenses/by/4.0/). The use, distribution or
reproduction in other forums is
permitted, provided the original
author(s) and the copyright owner(s)
are credited and that the original
publication in this journal is cited, in
accordance with accepted academic
practice. No use, distribution or
reproduction is permitted which does
not comply with these terms.

Zebrafish endochondral growth zones as they relate to human bone size, shape and disease

Pierre Le Pabic^{1*}, Daniel B. Dranow², Diego J. Hoyle²
and Thomas F. Schilling^{2*}

¹Department of Biology and Marine Biology, University of North Carolina Wilmington, Wilmington, NC, United States, ²Department of Developmental and Cell Biology, University of California, Irvine, Irvine, CA, United States

Research on the genetic mechanisms underlying human skeletal development and disease have largely relied on studies in mice. However, recently the zebrafish has emerged as a popular model for skeletal research. Despite anatomical differences such as a lack of long bones in their limbs and no hematopoietic bone marrow, both the cell types in cartilage and bone as well as the genetic pathways that regulate their development are remarkably conserved between teleost fish and humans. Here we review recent studies that highlight this conservation, focusing specifically on the cartilaginous growth zones (GZs) of endochondral bones. GZs can be unidirectional such as the growth plates (GPs) of long bones in tetrapod limbs or bidirectional, such as in the synchondroses of the mammalian skull base. In addition to endochondral growth, GZs play key roles in cartilage maturation and replacement by bone. Recent studies in zebrafish suggest key roles for cartilage polarity in GZ function, surprisingly early establishment of signaling systems that regulate cartilage during embryonic development, and important roles for cartilage proliferation rather than hypertrophy in bone size. Despite anatomical differences, there are now many zebrafish models for human skeletal disorders including mutations in genes that cause defects in cartilage associated with endochondral GZs. These point to conserved developmental mechanisms, some of which operate both in cranial GZs and limb GPs, as well as others that act earlier or in parallel to known GP regulators. Experimental advantages of zebrafish for genetic screens, high resolution live imaging and drug screens, set the stage for many novel insights into causes and potential therapies for human endochondral bone diseases.

KEYWORDS

Danio rerio, endochondral, skeleton, cartilage, growth plate

1 Introduction

Research on the growth plates (GPs) of endochondral bones in mice has greatly impacted our understanding of skeletal development as well as the causes of human skeletal disorders. Early studies showed that the epiphyses of limb long bones remain cartilaginous and proliferative, thereby allowing bone growth (1). Genetic studies showed

mechanisms regulating cartilage maturation, gradual replacement by osteoblasts, matrix deposition and continuous bone remodeling by osteoclasts (2). These discoveries laid the groundwork for much of modern skeletal research. Given the limited knowledge of the cellular and molecular mechanisms regulating the huge variety of sizes and shapes of other bones, such as those of the skull or vertebrae, much of our current understanding of skeletal development is based on work on GPs of long bones in the tetrapod limb.

Over the past several decades, the zebrafish has become a powerful system for genetic analysis of skeletal development. Despite having fins that lack the long bones found in tetrapod limbs and many other obvious anatomical differences in their skeletons, zebrafish have the same array of skeletal cell types found in humans. Furthermore, the work that has been done to date has shown that the molecular mechanisms that control skeletal development, growth and physiology are largely conserved despite over 400 million years since their lineages diverged from a common ancestor (3).

In this review, we present an overview of skeletal research in zebrafish with a special focus on endochondral growth zones (GZs), defined as regions of cartilage proliferation and maturation, which include the well-known GPs of long bones. For reviews covering other aspects of skeletal research in zebrafish (e.g. osteoblasts/osteoclasts, intramembranous skull bones, fin rays, scales), we refer the reader to the following (4–11). First, we provide a brief introduction to adult zebrafish skeletal anatomy with a specific focus on similarities with human endochondral bones. Next, we present the cellular architecture of GZs between zebrafish and humans and across the three major skeletal regions, cranial, axial and appendicular. Third, we compare endochondral development and physiology between zebrafish and mammals and review key recent studies that have led to insights into conserved cellular pathways that control bone size and shape in health and disease.

2 Skeletal anatomy in adult zebrafish and humans

2.1 Anatomical distribution of endochondral and intramembranous bones

2.1.1 Modes of ossification

Two modes of ossification produce the vertebrate skeleton: endochondral and intramembranous. In endochondral ossification, typified by long bones of the mammalian limb, mesenchymal condensations differentiate into cartilage that is eventually replaced by bone (2). In contrast, intramembranous bones, such as those of the skull vault, differentiate directly from mesenchyme (12). Some bones form by a combination of intramembranous and endochondral ossification, such as

mammalian clavicles (13). The relative contributions of these two modes of ossification vary widely across different taxa, both in the axial skeleton, which consists of bones associated with the craniofacial complex and vertebrae, as well as the appendicular skeleton that supports the limbs and fins (Figure 1). Human and zebrafish skulls are both composed of a mixture of endochondral and intramembranous bones (14). While the mammalian calvaria occupies a large surface area, the chondrocranium and pharyngeal skeleton are composed of many smaller endochondral bones, just as in zebrafish (14, 15). In contrast, most of the zebrafish vertebral and limb skeletons are intramembranous while they are endochondral in humans. Despite these differences, zebrafish and humans are generally very similar in their development and basic structure. However, homologies between individual axial and appendicular bones of teleost fish and humans can be difficult to determine due to phylogenetic divergence and adaptation to different environments.

2.1.2 Bones of the axial and appendicular skeletons

In the skull, difficulty in identifying homologous bones between humans and other vertebrates is thought to be partly a consequence of progressive fusion of skeletal elements during mammalian evolution (16). The human skull contains 29 bones, all joined by fibrous joints known as sutures, except for the mandible, hyoid bone, and middle ear ossicles (17). Two thirds of these cranial bones are intramembranous, while the hyoid bone, middle ear ossicles, and several bones of the cranial base (ethmoid, body and lesser wings of the sphenoid, petrous portion and otic capsule of the temporal bone, and basal portion of the occipital bone) are endochondral (Figure 1). In contrast, the zebrafish skull contains 134 bones, 78 of which are endochondral (14). As in humans, the intramembranous bones of the zebrafish braincase suture together, while bones supporting the jaws, opercle, gills and other parts of the skull, articulate with each other by mobile joints (Figure 1).

The non-cranial portion of the axial skeleton includes the vertebral column and rib cage in both humans and zebrafish, in addition to the unpaired fins (dorsal, anal, caudal) in zebrafish (Figure 1). Vertebrae and ribs are endochondral in humans but intramembranous in zebrafish (4, 18–20). In addition, unlike in humans, the zebrafish ribcage remains open ventrally and lacks a sternum. The zebrafish axial skeleton also includes appendages with no homologs in humans: the dorsal, anal, and caudal fins. Fins consist of an exoskeleton of rays made of intramembranous bone, and a supporting internal skeleton made of endochondral hypurals in the caudal fin and radials in the dorsal and anal fins (Figure 1B). Lastly, the Weberian apparatus, an evolutionary innovation linking the ear to the swim bladder to enhance audition (a character found only in the Ostariophysan superorder), contains both intramembranous and endochondral bones (21) (Figure 1B).

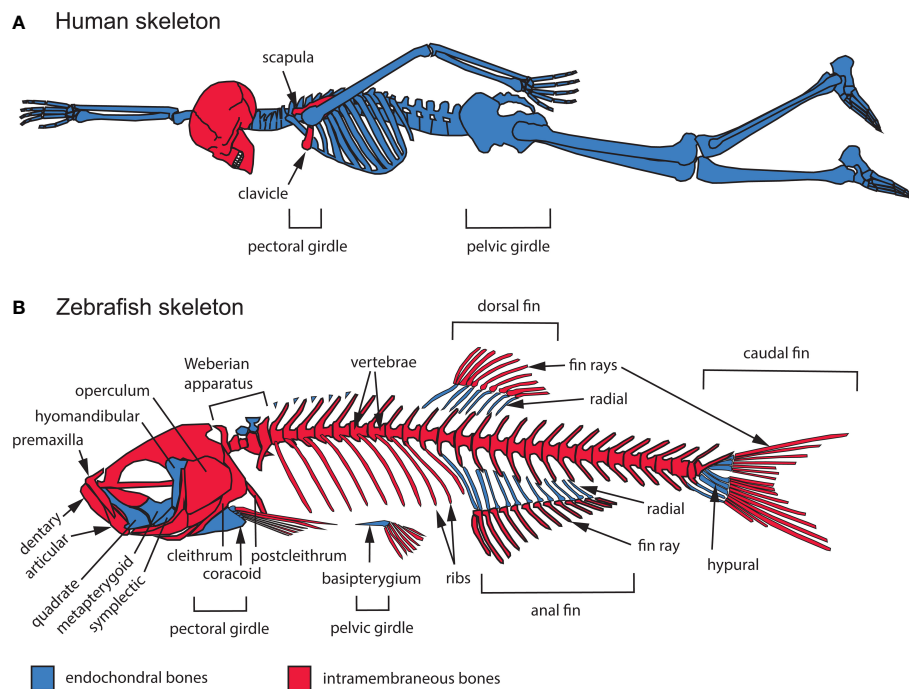


FIGURE 1

General overview of the intramembraneous and endochondral composition of the zebrafish and human skeletons. **(A)** Human adult skeleton. In the head, intramembraneous bones such as those of the calvaria (the top portion of the neurocranium) dominate the human skull in surface area, while endochondral bones mostly occupy the cranial base. All of the bones that compose the trunk and appendicular skeletons are endochondral, except for portions of the clavicle and scapula. **(B)** Zebrafish adult skeleton. The zebrafish skull, trunk and appendage skeletons are composed of both intramembraneous and endochondral bones. The zebrafish skull is composed of 134 bones, 78 of which are endochondral. The zebrafish trunk skeleton is composed of intramembraneous vertebrae and ribs. The zebrafish appendage skeleton is composed mostly of endochondral bones, while the fin ray exoskeleton is completely intramembraneous.

Human and zebrafish appendicular skeletons consist of pectoral (shoulder) and pelvic (hip) girdles with associated appendages: fore- and hindlimbs in humans, pectoral and pelvic fins in zebrafish. Human limbs are entirely composed of endochondral bones, while paired fins in zebrafish consist of fin rays made of intramembraneous bone supported proximally by endochondral radial bones (22). In humans, most of the pectoral and pelvic girdles are also endochondral, though portions of the clavicle (collar bone) and scapula (shoulder blade) form by intramembraneous ossification (Figure 1A). Similarly, the zebrafish pectoral girdle contains a mixture of intramembraneous (cleithrum, postcleithrum, supracleithrum) and endochondral (coracoid, mesocoracoid, scapula) bones, while the pelvic girdle is exclusively endochondral (basipterygium) (14).

2.2 Endochondral growth zone structure

2.2.1 Cellular architecture of endochondral growth zones

In endochondral GZs, step-by-step chondrocyte maturation regulates bone elongation (Figure 2) (1). The maturation process

starts in the resting zone (RZ), which serves the role of stem-cell niche (Figure 2A). Slow-dividing RZ cells transit into the proliferative zone (PZ), where they proliferate at a higher rate and stack to form chondrocyte arrays characteristic of avian and murine long bone GPs. They subsequently stop dividing and enlarge as they enter the hypertrophic zone (HZ). Most undergo apoptosis at the chondro-osseous junction and are subsequently replaced by bone. In GPs with steady-state growth, pools of cells in each zone remain constant as: 1) the rate of PZ cell division offsets the rate of cells leaving the PZ, 2) the rate of cells leaving offsets the rate of cells entering the PZ, and 3) the rate of cells entering the HZ offsets the rate of cells lost at the chondro-osseous junction (25). These aspects of cartilage maturation appear broadly similar between mammalian and zebrafish endochondral GZs, though chondrocytes are not aligned into linear stacks in zebrafish PZs (26, 27).

Cartilage maturation can occur in one or both directions at GZs, parallel to the long axis of bone growth. In unidirectional (or epiphyseal) GZs (also known as GPs) typical of long bones, the RZ lies close to the distal-most region of the bone (epiphysis) and maturing cells progress medially toward the bone's central shaft (diaphysis), producing axial elongation at each end (1). In contrast,

bidirectional GZs produce growth in two opposite directions (28). This reflects a mirror-image organization where two sets of PZs and HZs flank a single RZ on either side (Figure 2B). Bidirectional GZs are often located within synchondroses or cartilaginous joints. In humans, they can be found in the skull base and vertebrae but in zebrafish are more common and found in multiple endochondral bones of the neurocranium and pharyngeal skeleton (Figure 3) (27).

2.2.2 Tissue architecture of endochondral bones

Although both human and zebrafish endochondral bones have GZs, they show several structural differences, including the fact that zebrafish lack: 1) secondary ossifications, 2) trabecular bone, and 3) a hematopoietic bone marrow (Figure 2). Human GPs often have “secondary” ossification centers distal to the RZ,

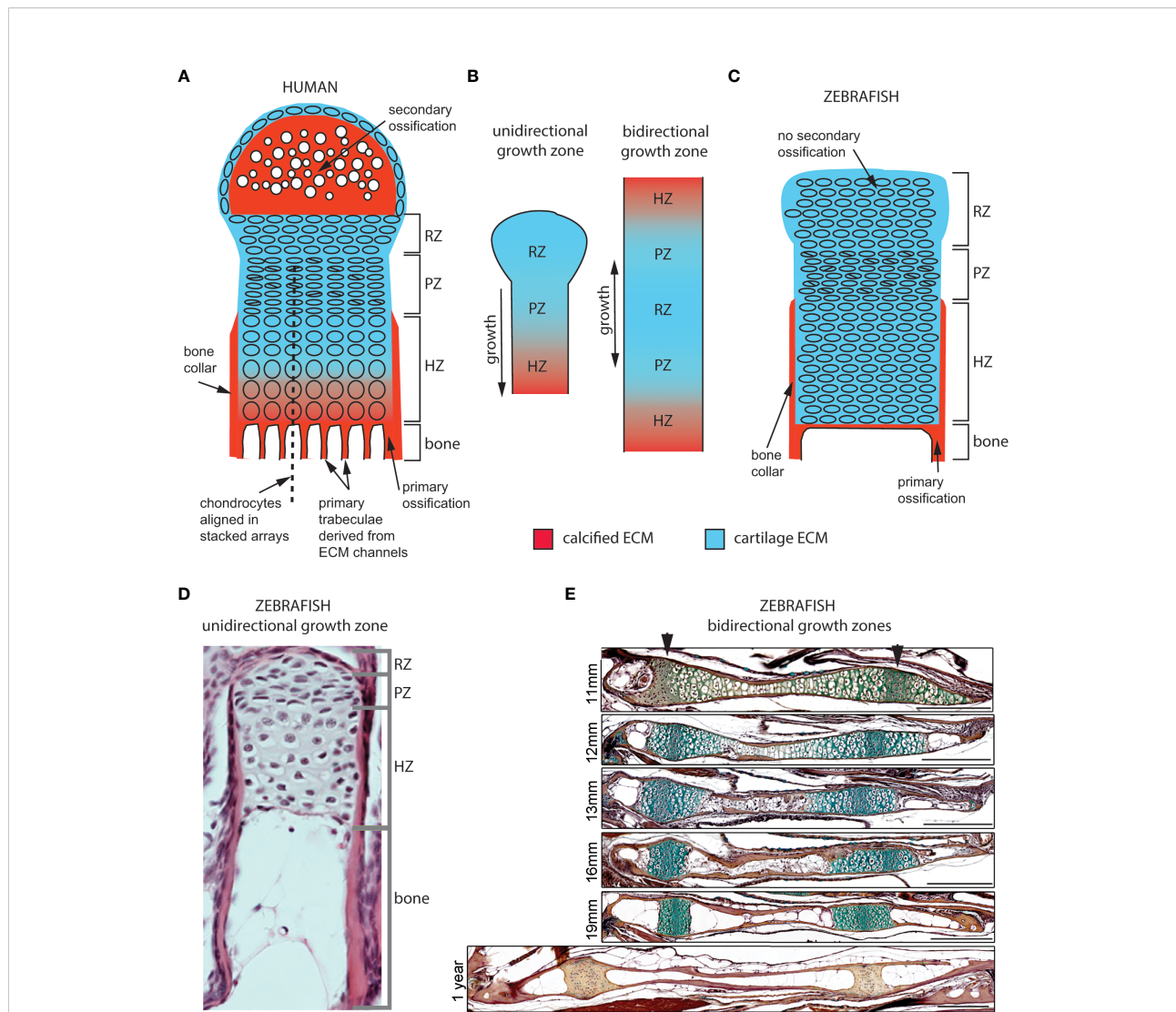


FIGURE 2

Cellular organization of epiphyseal and synchondrosal growth zones. (A) Human growth plate chondrocytes transition through resting-, proliferative- and hypertrophic zones (RZ, PZ, and HZ, respectively) before dying or transitioning to an osteoblast fate at the chondro-osseous junction. Cartilage cells stop dividing and enlarge in the hypertrophic zone. The bone collar forms a sheath around hypertrophic chondrocytes; the secondary ossification flanks the growth plate distally. Primary bone trabeculae derived from extracellular matrix channels populate the bone cavity. (B) In unidirectional (epiphyseal) growth zones, the resting zone is distal to the proliferative zone, itself distal to the hypertrophic zone; this layout produces unidirectional growth. In bidirectional (synchondrosal) growth zones, the resting zone is flanked by two proliferative zones and two hypertrophic zones in a mirror image organization; this layout produces bidirectional growth. (C) Stereotypical zebrafish unidirectional growth zone organization: chondrocytes transition through RZ, PZ and HZ, but they do not enlarge in the HZ. At the zebrafish resorption front, chondrocytes die or transition to either an osteocyte or adipocyte fate. A perichondral bone collar sheathes the zebrafish hypertrophic zone, but no secondary ossification is associated with zebrafish epiphyseal growth zones. Trabeculae are not observed in smaller teleosts such as zebrafish. (D) Histological section of zebrafish proximal radial showing unidirectional endochondral growth zone [originally published in (23)]. (E) Time series of maturation at two zebrafish bidirectional growth zones located within the ventral (left) and dorsal (right) ceratohyal synchondroses [originally published in (24)]. (scale bars = 50 μm).

which appear later in endochondral differentiation (Figure 2A) (2). In contrast, in zebrafish and other teleost GZs, maturing cartilage remains continuous with articular cartilage at the joints, similar to earlier stages of mammalian GP development (Figures 2C–E) (27, 29, 30). Secondary ossification centers in mammals were recently proposed to have evolved to protect hypertrophic chondrocytes from mechanical damage in load-bearing tetrapod bones (31). Another striking structural difference from mammals is the absence of primary bone trabeculae at the resorption front in zebrafish (32, 33). Primary trabeculae form parallel bone channels in mammals through the progressive replacement of extracellular matrix (ECM) tracks produced by chondrocyte stacks by bone ECM (Figure 2A), while secondary trabeculae appear later in response to mechanical stress (34, 35). Thus, the less well-aligned chondrocyte stacks of zebrafish GZs as well as the lower amount of ECM produced by GZ chondrocytes (also observed in other teleosts) may help explain the lack of primary trabeculae (Figures 2C–E) (29, 30, 36). However, trabeculae have been reported in the bones of larger teleosts, suggesting that their presence might simply reflect differences in bone size and strength requirements (37). In addition, zebrafish HZ chondrocytes are converted into osteoblasts at the resorption front, become part of the diaphyseal endosteum and differentiate into osteocytes embedded in the bone shaft (24). This supports the presence of endochondral ossification in zebrafish in the form of (1): a thin layer of bone matrix at the resorption front and (2) bone matrix deposition inside the bone shaft, instead of the bone spongiosa described in mammals and larger teleosts (24, 32, 37). Finally, zebrafish endochondral bones do not form a marrow that can support hematopoiesis. This instead occurs in the kidney marrow of zebrafish (38).

2.3 Anatomical distribution of endochondral growth zones

Rodents and humans have homologous skeletal GZs inherited from a shared common ancestor, as exemplified by long bone GPs such as the proximal tibial GP. Though zebrafish GZs are not individually homologous to any mammalian GZ, a growing body of research has revealed striking similarities in their GZ development and physiology. This demonstrates the relevance of zebrafish for understanding basic principles of skeletal biology and underlying causes of skeletal disease, including common chondrodysplasias associated with GPs. These similarities include the molecular and cellular mechanisms underlying endochondral differentiation. The genetic advantages of the zebrafish, along with its small size and optical accessibility, has led to a growing popularity for their use in testing new disease candidates discovered in humans and elucidating their mechanisms of action.

2.3.1 Bidirectional endochondral growth zone locations

Postembryonic growth of the human cranial base requires three bidirectional GZs: the spheno-ethmoidal, intersphenoid and spheno-occipital synchondroses (Figure 3A). Their importance in shaping the adult face is exemplified by the prominent forehead and flattened bridge of the nose associated with achondroplasia, the most common form of human dwarfism (39, 40). Reduced cell proliferation in the RZ of these GZs in achondroplasia results in reduced cranial base growth in patients, in addition to shortening of their arms and legs due to GP defects (Figure 3B) (41). The other anatomical location where bidirectional growth zones are found in humans are the vertebrae. Neurocentral synchondroses contribute to the growth of the vertebral body as well as the spinal canal (Figure 3B), and they fuse between ages 5 to 17 depending on their anterior-posterior location (42).

Zebrafish bidirectional growth zones are primarily located in the neurocranial and pharyngeal skeletons. As in mammals, the zebrafish neurocranium consists of both intramembranous and endochondral bones and numerous neurocranial synchondroses arise after the initial stages of chondrocranial ossification, yet their GZ activity has only recently been investigated (27). Growth of the zebrafish pharyngeal skeleton is supported by both uni- and bidirectional growth zones (Figure 3C). The pharyngeal skeleton derives from the pharyngeal arches (PA), which form by bilateral segmentation of the embryonic pharynx in vertebrates and their close relatives (16, 43, 44). Here we describe the PA-derived bidirectional GZs of the first (PA1, mandibular) and second (PA2, hyoid) arches, which develop first and produce the most skeletal growth, as these are most relevant to model human GZs in health and disease. For a more complete list of zebrafish pharyngeal GZs, see (27). In the dorsal PA1 skeleton, the palatoquadrate (PQ) synchondrosis mediates growth of the quadrate (QA) ventrally and metapterygoid (MP) dorsally (Figure 3C). In the dorsal PA2 skeleton, the hyosymplectic (HS) synchondrosis mediates growth of the symplectic (SY) ventrally and hyomandibular (HM) dorsally. In the ventral PA2 skeleton, the ventral ceratohyal (CH) synchondrosis mediates growth of the hypohyal (HH) bones ventrally and the CH dorsally, while the dorsal CH synchondrosis mediates growth of the CH (anterior CH) ventrally and epihyal (EH; posterior CH) dorsally (Figure 3C). In the PA3-6 (branchial arches 1-4) skeleton, basibranchial (BB) elongation is mediated by 2 bidirectional GZs (Figure 3C) (27).

The zebrafish PQ and CH synchondroses have been used to study developmental mechanisms that regulate GZ development (24, 26, 45, 46). These studies have shown that, like mammalian GPs, these GZs contain similar zones of cartilage maturation (RZ, PZ, HZ), though with some interesting differences in the timing of proliferation and hypertrophy. In addition, they share similar patterns of gene expression known to control GZ formation and size, as discussed below.

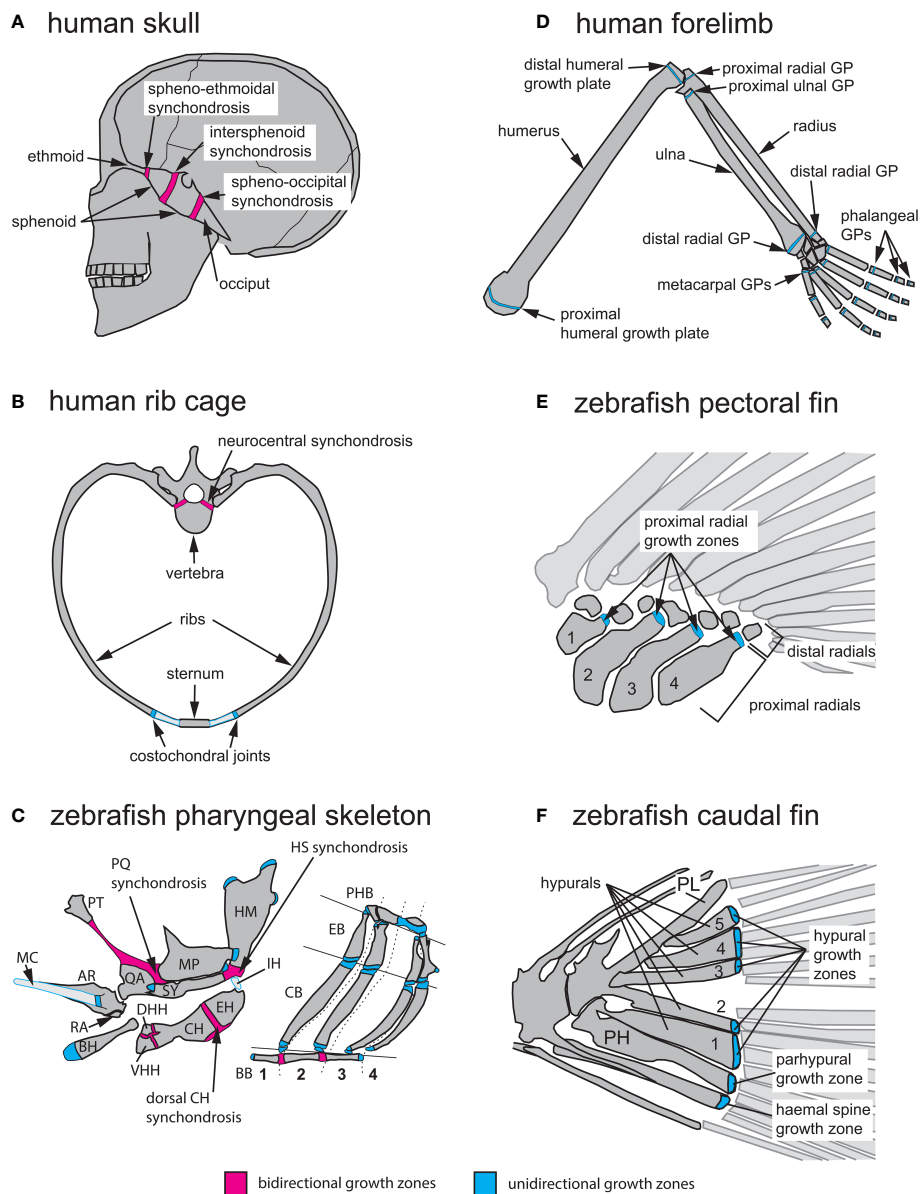


FIGURE 3

Anatomical locations of endochondral growth zones in human vs zebrafish. **(A)** Three synchondroses mediate growth of the human skull base (depicted in sagittal view): the sphenothmoidal-, intersphenoid- and sphenoccipital synchondroses. **(B)** Endochondral growth of human vertebrae and ribs (depicted in transverse view) takes place at neurocentral synchondroses and costochondral joints, respectively. **(C)** Over thirty endochondral growth zones mediate zebrafish pharyngeal skeleton growth. Three highly visible synchondroses mediate growth of first and second pharyngeal arch (PA1-2) skeletons. The PQ synchondrosis mediates growth of the QA and MP. The HS synchondrosis mediates growth of the SY and HM. The dorsal CH synchondrosis mediates growth of the CH and EH. In PA1 and 2, epiphyseal growth zones are found at the posterior MP, anterior SY, dorsal HM and anterior BH. In the gill supporting skeleton, epiphyseal growth zones are found at the ends of each CB and EB bone. **(D)** Axial growth of human stylopod (humerus, femur) and zeugopod (radius, ulna, tibia, fibula) bones is mediated by epiphyseal growth zones (=growth plates) located at each bone extremity. A single proximal epiphyseal growth zone mediates axial elongation of each autopod long bone (hand and foot phalanges). **(E)** In the zebrafish pectoral fin, epiphyseal growth zones are found at the distal end of each proximal radial. **(F)** In the zebrafish caudal fin, epiphyseal growth zones located at the distal end of each hypural bone (H1-5), the prehypural and two last haemal spines mediate axial elongation. AR, articular; BB, basibranchials; BH, basihyal; CB, ceratobranchial; CH, ceratohyal; DHH, dorsal hypohyal; EB, epibranchial; EH, epihyal; HM, hyomandibular; HS, hyosymplectic; IH, interhyal; MC, Meckel's cartilage; MP, metapterygoid; PH, parhypural; PHB, pharyngobranchials; PL, pleurostyle; PT, palatine; QA, quadrate; RA, retroarticular; SY, symplectic; VHH, ventral hypohyal. Red indicates bidirectional- and blue indicates unidirectional growth zones.

2.3.2 Unidirectional endochondral growth zone locations

In humans, unidirectional GZs are primarily found in the limbs and ribs (Figures 3B, D). Growth of ribs is mediated by GZs located within costochondral joints, which are synchondroses linking ribs to the costal cartilages of vertebrae (Figure 3B) (47, 48). In the limbs, epiphyseal GPs mediate elongation of the stylopod (humerus, femur) and zeugopod (radius/ulna, tibia/fibula) at the end of each long bone. In contrast, each bone of the autopod grows at a single GP (phalanges/metacarpals/metatarsals; Figure 3D).

Zebrafish unidirectional GZs are primarily found in the pharyngeal skeleton and fin endoskeleton (Figures 3C, E, F). In the PA3-6 (branchial arches 1-4) skeleton, the ceratobranchial (CB) and epibranchial (EB) bones of each arch possess a unidirectional GZ at each extremity (Figure 3C) (27). In the 2 sets of paired fins (pectoral and pelvic) the endoskeleton is reduced compared to that of human limbs, and its proximo-distal pattern is simplified. The endoskeleton of pectoral fins consists of 4 proximal radials and 6 to 8 distal radials (Figure 3E), while the pelvic fins contain 3 radials (22). The caudal fin endoskeleton consists of the pleurostyle of the caudal-most vertebrae, five hypurals, the parhypural, and the haemal spines of preural vertebrae 2 and 3 (Figure 3F) (49). Just as in mammalian limbs, all fin GZs are unidirectional. These are positioned at the distal ends of (1) proximal radials in the pectoral, dorsal and anal fins (2), radials in the pelvic fins, and (3) hypurals, parhypural and haemal spines in the caudal fin (Figures 3E, F) (50). Interestingly, mutations in conserved regulators of appendage development can lead to supernumerary bones in zebrafish consistent with radials and long bones having evolved from homologous structures in the common ancestor (23).

3 Development and cellular architecture of endochondral growth zones in teleost fish and humans

3.1 Developmental similarities and differences in endochondral growth zones between species

The stereotypical steps of mammalian endochondral long bone formation consist of: 1) mesenchymal condensation, 2) differentiation into cartilage, 3) formation of a perichondral bone collar at the diaphysis and concomitant hypertrophy of chondrocytes coupled with cartilage matrix mineralization, 4) blood vessel invasion, hypertrophic chondrocyte death and resorption of mineralized matrix by chondroclasts, all at the

diaphysis 5) replacement of cartilage by endochondral bone and marrow, 6) appearance of distinct RZ, PZ, and HZ zones at each epiphysis, and lastly 7) epiphyseal formation of secondary ossification centers (2, 12). These features of GZs are largely conserved between teleost fish and tetrapods, at both the cellular and molecular levels, despite the later invasion of blood vessels in teleosts, lack of hematopoietic bone marrow or secondary ossifications. Notably, endochondral bone formation in smaller teleosts, such as zebrafish takes the form of (1) a thin layer of bone matrix at the resorption front and (2) bone matrix deposition on the inner surface of the bone shaft (24, 29, 30, 32, 36, 51).

3.1.1 From condensation to cartilage template

In tetrapods, the shape of the mesenchymal condensation determines the shape of the cartilage model (52). In contrast, cartilage elements differentiate within larger condensations in both the head and fins of teleosts (22, 53–55). Zebrafish embryonic and larval cartilage shapes generally prefigure the shape of adult skeletal elements (Figures 4A, B). One exception is the endoskeleton that supports the pectoral fins, in which a transient endoskeletal disc of cartilage supports the functional larval fin, but localized cartilage decomposition within the disc defines four proximal radials that prefigure the adult fin endoskeleton (Figures 3E, 4C) (56).

The shapes of pharyngeal cartilage elements in teleost embryos are regulated by complex morphogenetic cell behaviors such as localized cell-cell intercalations that take place hours before cartilage matrix deposition (56–59). Linear stacking of chondrocytes driven by such intercalations underlies the directionality of the GP or GZ as well as cartilage and bone elongation. Cartilage elements of mutants with cell-cell intercalation defects are shorter and wider than in wild-type individuals (26, 60). A growing body of research supports conserved control of cell-cell intercalation during cartilage morphogenesis in the RZs of vertebrate GPs (including mammals) by planar cell polarity (PCP) pathways (26, 58, 60–66).

Though initially studied in the context of epithelia, it has become clear that noncanonical Wnt/Wnt-PCP and Fat-Dchs/Fat-PCP signaling play important roles in regulating cell and tissue polarity in diverse cell and tissue types, including mesenchyme and cartilage. Several human syndromes that affect skeletal morphology are caused by mutations in Wnt-PCP and Fat-PCP signaling genes (67–77). Studies in zebrafish have successfully modeled craniofacial defects associated with loss-of-function of *gpc4*, *frizzled*, *wnt5b*, *fat3a* and *dchs2* in cartilage morphogenesis, and demonstrated requirements for these factors in mediating the polarized cell-cell intercalation of chondrocytes in the craniofacial skeleton (26, 58, 63, 64, 66).

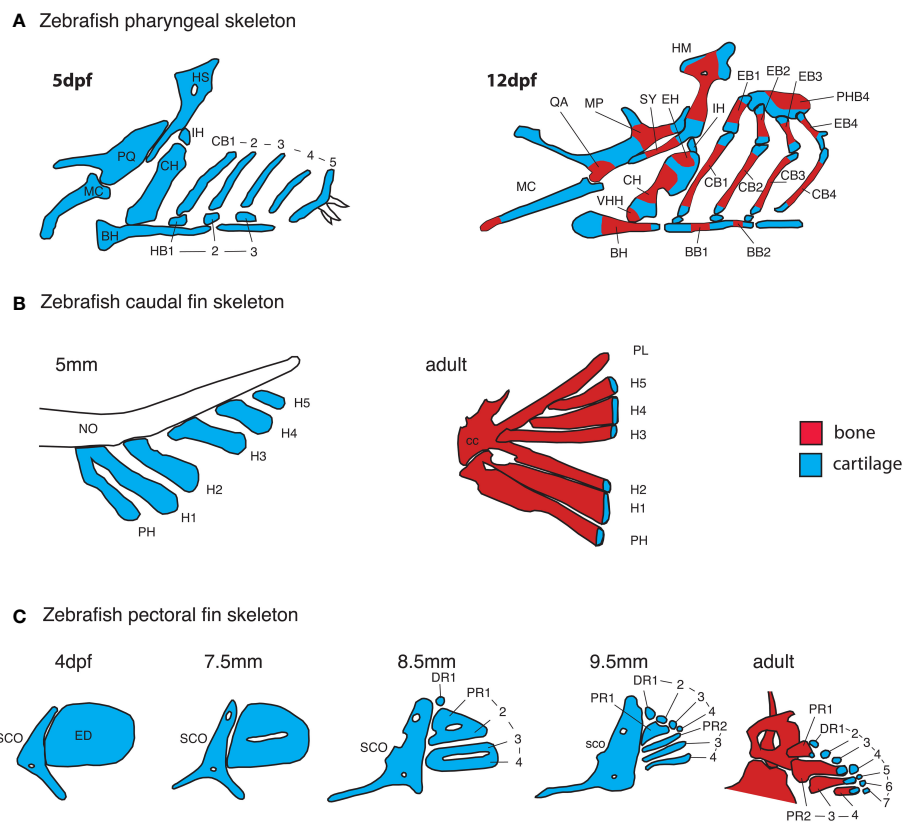


FIGURE 4

Early anatomy of zebrafish endochondral growth zones. **(A)** Endochondral growth zones start to appear in the zebrafish skeleton around 12 days post-fertilization (dpf). One or more ossification centers appear on each bone. Unossified cartilage regions at bone ends become unidirectional growth zones, while those flanked by ossifying cartilage become bidirectional growth zones. In the 12 dpf pharyngeal skeleton, the QA and MP bones ossify over the PQ cartilage, the HM and SY bones ossify over the HS cartilage, the HH, CH and EH bones ossify over the CH cartilage, BB1 and 2 ossify over the BB cartilage. Single ossifications appear on other pharyngeal bones. **(B)** In the caudal fin endoskeleton, single ossifications appear on each cartilage element, resulting in a single distal endochondral growth zone per element. **(C)** In the pectoral fin endoskeleton, the endoskeletal disc is progressively carved into four proximal- and seven distal radials. Ossification of each proximal radial leaves a single endochondral growth zone at the distal end. Distal radials do not ossify. BB, basibranchial; BH, basihyal; CB, ceratobranchial; CC, compound centrum; DR, distal radial; ED, endoskeletal disc; H, hypural; HB, hypobranchial; IH, interhyal; MC, Meckel's cartilage; NO, notochord; PH, parhypural; PHB, pharyngobranchials; PR, proximal radial; SCO, scapulocoracoid; VHH, ventral hypohyal.

3.1.2 Maturation of endochondral bones

The first signs of GZ development in the craniofacial skeleton in zebrafish are the simultaneous appearance of a perichondral bone collar and flattening of presumptive PZ chondrocytes during early metamorphosis (Standard Length = 6–7 mm) (26, 27). Unlike mammalian GZs, hypertrophic chondrocytes in zebrafish only enlarge slightly and transiently during zebrafish GZ development. Blood vessel invasion of the cartilage template coincides with the onset of HZ cell apoptosis, but unlike in mammals, it starts well after the onset of bone collar formation and GZ-mediated bone elongation (24, 27). It was long thought that osteocytes replacing HZ chondrocytes in GPs were introduced in the bone diaphysis by invading vasculature (2), but histological studies in chick and more recent lineage analyses using transgenic mice have shown a contribution to trabecular bone by HZ chondrocytes themselves

(78–81). Similarly, recent clonal analysis using zebrafish transgenics has shown that HZ chondrocytes may undergo several fates at the resorption front: apoptosis, or transition into osteoblast or adipocyte fates (24). Unlike mammals, but similar to amphibians, reptiles and most bird species, secondary ossification centers do not develop in GZs of endochondral bones in zebrafish or other teleosts (1, 27, 29, 30).

3.1.3 Patterning of endochondral growth zones

Our understanding of GZ patterning mechanisms is largely based on studies of mouse limb GPs. Two signaling pathways activated by Indian Hedgehog (Ihh) and Parathyroid Hormone-like Hormone (Pthlh), respectively, interact at a distance to pattern long bone GPs (Figure 5A). *Ihh* is first expressed throughout the diaphysis of long bone cartilage templates before becoming restricted to chondrocytes in the pre-

hypertrophic zone (PHZ) (82, 86). *Ihh* activates *Pthlh* expression at a distance in periarticular chondrocytes, and *Pthlh* in turn represses *Ihh* expression. Mosaic analyses of *Ihh*, *Pthlh*, and *Pth1r* mutants have shown that this negative feedback loop effectively patterns the distance between RZ and HZ (83, 84). *Ihh* expression levels are also regulated by BMP and FGF signaling: *Smad1/5* promotes *Ihh* expression, while *Smad2/3* and *Egfr3* repress its expression (87–90). In addition to their role in scaling the GP, *Ihh* promotes bone collar formation by inducing the differentiation of osteoblasts in the perichondrium (91, 92), while *Pthlh* promotes the proliferation of PZ chondrocytes and delays cell-cycle exit and the onset of chondrocyte enlargement, both in mice and zebrafish (82, 92). In contrast, little is known about the molecular pathways regulating HZ chondrocyte enlargement. Three phases of enlargement have been identified in mice, which include an initial three-fold volume increase through hypertrophy, that is, cell enlargement with a corresponding increase in organelle dry mass, followed by a four-fold increase through vacuole swelling by disproportionate intake of fluid, and a final two-fold increase through hypertrophy again. Interestingly, the duration of the last phase (hypertrophy) varies the most between rapidly and slowly expanding growth plates, and regulation of this phase requires *Insulin-like growth factor 1 (Igf1)* (93).

The *Ihh*-*Pthlh* feedback loop appears to be conserved in mammalian cranial base synchondroses, although *Pthlh* is expressed throughout the RZ and PZ (94, 95). A few studies in zebrafish have shown the conservation of GZ patterning mechanisms between teleost fish and mammals (45, 96), and an earlier onset of *Pthlha* expression than previously described, namely at the onset of chondrogenesis and before the onset of *ihha* expression (Figure 5B) (46). Novel findings in zebrafish have also shown the potential of this model for expanding our understanding of GZ patterning, as they suggest that the *Ihh*-*Pthlh* feedback loop maintains but does not establish the GZ pattern, at least in some pharyngeal endochondral bones (46). Instead, the zebrafish *Pthlh* ortholog, *pthlha*, and mechanical force from muscle contraction initiate the HZ and the location of subsequent *ihha* expression, thereby establishing the negative feedback-loop that maintains GZs (Figure 5B) (46).

3.2 Cellular basis of similarities and differences in endochondral growth zones between species

3.2.1 Bone elongation and differential growth

The rate of bone elongation changes throughout the life of a GZ, and differs between GZs of an individual, as well as homologous GZs of different species. Such growth rate variation is referred to as differential growth (1). In rats,

three cellular mechanisms mediate endochondral bone elongation: cell proliferation, cell enlargement, and ECM production. Cell proliferation takes place in the PZ and enlargement in the HZ, while ECM production takes place in both zones. These three cellular mechanisms contribute unequally to bone elongation in mammalian GPs: proliferation 7–10%, ECM production 32–49%, and cell enlargement 44–59% (25). The relatively minor contribution of proliferation to growth serves to compensate for the loss of chondrocytes at the chondro-osseous junction. Between mammalian species, as shown for bat metacarpal and jerboa metatarsal GZs, the largest driver of growth rate is the degree of cell enlargement of HZ chondrocytes (93, 97). In contrast, proliferation is the major contributor to endochondral bone elongation in zebrafish, as no significant cell enlargement or increase in ECM content are observed in active GZs (27). In other teleost fishes, the cellular basis of endochondral growth has been explored in several African cichlids: ECM production is the main driver of growth in *H. elegans*, while differences in cell proliferation and/or enlargement mediate differential growth in Lake Malawi cichlids (98, 99).

3.2.2 Life history differences

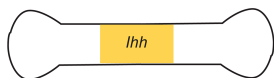
Mammals and teleost fishes also differ dramatically in the timing of growth over their lifespans. Human limb GPs are already active at birth and mediate axial elongation until the end of puberty, when estrogens trigger GP closure and growth arrest through complete replacement of epiphyseal cartilage by bone (100). In rats, GPs also become inactive at sexual maturity but they are not replaced by bone (1). Not all GPs become inactive at the same age: in humans, the three GZs of the cranial base ossify at different times: the intersphenoid GZ ossifies immediately before birth, the spheno-ethmoidal GZ ossifies at 6 years, and the spheno-occipital GZ remains active until the end of puberty (101–103). In contrast, most teleost fish grow throughout life, although the rate of growth slows with age, as described by the individual growth model of von Bertalanffy (104). Accordingly, zebrafish growth is indeterminate (105, 106), yet its pharyngeal GZs become inactive in adults and do not ossify, similar to rats. Further adult growth is mediated by intramembranous ossification (27).

3.3 Modeling human endochondral growth zone disorders in zebrafish

Despite the many similarities in development and physiology of their GZs, there have been relatively few studies modeling human GZ disorders in zebrafish. Recent reviews

A GZ PATTERNING IN MAMMALS

1. *Ihh* expression in diaphysis



2. *Ihh* activates *Pthlh* expression in epiphyses



3. *Ihh/Pthlh* feedback loop scales GZs

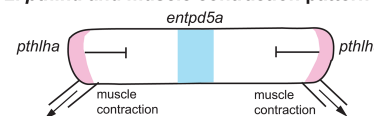


B GZ PATTERNING IN ZEBRAFISH

1. *pthlha* expression in epiphyses



2. *pthlha* and muscle contraction pattern GZs

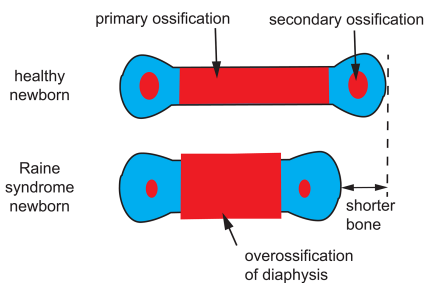


3. *ihh/pthlha* feedback loop maintains GZs

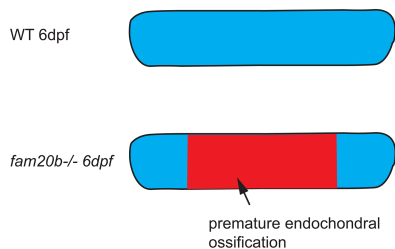


C OSTEOSCLEROTIC BONE DYSPLASIA

Human condition

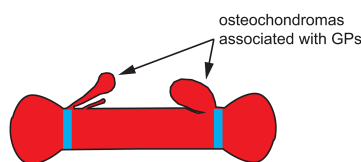


Zebrafish model



D HEREDITARY MULTIPLE EXOSTOSIS

Human condition



Zebrafish model

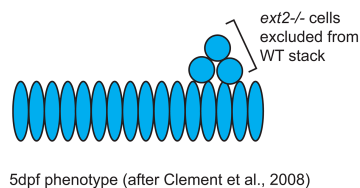


FIGURE 5

Zebrafish models of endochondral growth zone development and disease **(A)** Model for the patterning of growth zones (GZs) based on genetic studies of mouse long bones (82–84). *Indian hedgehog* (*Ihh*) is first expressed in the nascent diaphysis of the cartilage model. Its expression domain expands towards the epiphyses and activates *Parathyroid hormone-like hormone* (*Pthlh*) expression in periarticular cartilage. *Pthlh* represses *Ihh* at a distance, which sets the distance between the hypertrophic zone (HZ) and resting zone (RZ). **(B)** Model for the patterning of CH GZs in zebrafish based on (46). *pthlha* is expressed at the epiphyses of the differentiating CH. The HZ is then patterned by *pthlha* and muscle contractions before the onset of *ihha* expression. According to this model, *ihha* plays a role in the maintenance of GZs, not their patterning. **(C)** Zebrafish *fam20b* mutants recapitulates the skeletal phenotype of Rainie syndrome, a particular form of osteosclerotic bone dysplasia (45). Short overossified long bones are observed in Rainie syndrome newborns. Premature ossification of the CH diaphysis is observed in zebrafish *fam20b* mutants. **(D)** Zebrafish chimaeras recapitulate the formation of cartilage nodules observed in the human condition hereditary multiple exostosis, which results from a mutation in the *EXT2* gene. *ext2*^{-/-} chondrocytes are excluded from WT cartilage stacks in zebrafish chimaeras, leading to the hypothesis that osteochondromas observed in *EXT2*^{+/-} patients result from loss-of-heterozygosity (85). *Ihh* and *ihha* expression domains in yellow, *Pthlh* and *pthlha* expression domains in pink, *ectonucleoside triphosphate diphosphohydrolase 5a* (*entpd5a*) expression domain in light blue, cartilage in blue, and bone in red. CH, ceratohyal; GPs, growth plates; WT, wild type; dpf, days post-fertilization.

largely focus on the many models for other types of bone diseases such as osteogenesis imperfecta, osteoporosis, osteopetrosis and osteoarthritis, that alter ossification and osteoblasts (4–10). Notable exceptions include mutations in genes encoding proteoglycan core proteins or enzymes involved in their biosynthesis or assembly, as models for such cartilage diseases as Keipert syndrome (Glypican 4, GPC4; discussed in section 1a), osteosclerotic bone dysplasia (FAM20C), and hereditary multiple exostoses (Exostosin 2, EXT2).

Zebrafish provided some of the first insights into requirements for proteoglycans in craniofacial development (45, 96). A variety of Human conditions result from mutations in the proteoglycan biosynthesis pathway that builds chondroitin-sulfate- (CSPGs) and heparin-sulfate-proteoglycans (HSPGs) from UDP-glucose. Zebrafish mutants in seven of the nine enzymes of the O-linked-glycosylation pathway required for HSPG production have been described, several of which recapitulate endochondral skeletal defects of human patients (107).

A surprising discovery associated with the cartilage phenotypes of zebrafish mutants in *UDP-xylose synthase* (*uxs1*), *xylotransferase 1* (*xylt1*) and *glycosaminoglycan xylosyl kinase* (*fam20b*) is the premature maturation of hypertrophic chondrocytes and bone collar ossification (Figure 5C). This suggested a role for proteoglycans in regulating the timing of cartilage and bone differentiation, perhaps through the modulation of ligand-based cell-cell signaling (45, 96). Further, premature ossification in *fam20b* mutants provided a new etiology for Raine syndrome, a human disease resulting from mutations in *FAM20C*. Also known as osteosclerotic bone dysplasia, Raine syndrome patients have craniofacial defects such as low nasal bridge and midfacial hypoplasia indicative of defects in growth at synchondroses, as well as short and overossified long bones in newborns (Figure 5C). The zebrafish *fam20b* mutant phenotype suggests that Raine syndrome craniofacial and limb skeletal defects result from premature maturation of the skeleton (45).

Further down the HSPG biosynthetic pathway, *exostosin* (*ext*) -1 and -2 code for glycosyltransferases involved in the polymerization of heparan sulfate chains. Mutations in *EXT1* or *EXT2* result in hereditary multiple exostoses (HME) in humans, a disease that causes the formation of benign bone tumors (osteochondromas) that are associated with GPs (Figure 5D). Most HME patients are heterozygous for mutations in either *EXT1* or *EXT2* (108–110). A study of zebrafish *ext2* mutants (*dackel*) supports a model where osteochondromas arise from local loss of heterozygosity (LOH): zebrafish *ext2*^{-/-} embryos do not develop

osteochondromas but their skeleton is generally misshapen, demonstrating a requirement for *ext2* in cartilage morphogenesis/stacking (85). Instead, *ext2*^{-/-} cells form osteochondroma-like nodules when transplanted in wild type (WT) individuals: homozygous mutant cells are excluded from WT stacks, providing support to the LOH model for the etiology of HME (Figure 5D) (85).

4 Conclusions and future directions

In this review, we have highlighted the many similarities and differences between zebrafish and human skeletal anatomy, their endochondral GZs and recent studies of developmental and physiological mechanisms that control endochondral bone growth. Despite the apparent anatomical differences between human and teleost fish skeletons, the overwhelming conservation of different cell types and molecular mechanisms underlying skeletal development makes the zebrafish a powerful model for further studies of the causes and potential therapies for human skeletal diseases. This power lies in (1): the unique and well-known properties that have already made zebrafish a popular model system, which include ease of care, their small size, large number of offspring, suitability for large forward genetic screens and embryo transparency to name a few and (2) an ever-expanding toolkit to reach a diversity of research goals. CRISPR-Cas9-mediated mutagenesis is relatively easy in zebrafish and protocols have been developed for the rapid production of loss-of-function phenotypes in CRISPR-injected individuals (111, 112). Numerous transgenic lines labeling various skeletal cell lineages and their precursors have been used to image cartilage and bone morphogenesis *in vivo*, and also conduct lineage tracing in endochondral bones (24, 58, 113, 114). Transgenic zebrafish can also be utilized for cell-type and stage-specific ablation using the nitroreductase system (115), as well as in mosaic transgenic conditions to test the cell-autonomous and non-cell autonomous properties of particular genes and their mutant alleles (46, 116, 117). Lastly, recent improvements in single-cell RNAseq and ATACseq methodologies have allowed gene expression profiling of entire cell lineages and even whole organs or organisms at single cell resolution, made possible by the small size of zebrafish embryos and larvae (118–122). Future deployment of these single-cell techniques for the study of all skeletal cell types will undoubtedly lead to new insights into endochondral and GZ development in health and disease.

Author contributions

PL, DD, DH and TS all contributed to the conception and content covered in the manuscript. PL wrote the first draft of the manuscript. TS wrote sections of the manuscript. All authors contributed to manuscript revision, read, and approved the submitted version.

Funding

The authors of this work were supported by National Institutes of Health awards R01 DE013828 and R01 DE030565, as well as a National Science Foundation award MCB 2028424.

References

- Farnum C. *Postnatal growth of fins and limbs through endochondral ossification*. Chicago, IL, USA: University of Chicago Press (2007). p. 118–51.
- Kronenberg HM. Developmental regulation of the growth plate. *Nature* (2003) 423(6937):332–6. doi: 10.1038/nature01657
- Hurley IA, Mueller RL, Dunn KA, Schmidt EJ, Friedman M, Ho RK, et al. A new time-scale for ray-finned fish evolution. *Proc R Soc B-Biological Sci* (2007) 274(1609):489–98. doi: 10.1098/rspb.2006.3749
- Tonelli F, Bek JW, Besio R, De Clercq A, Leoni L, Salmon P, et al. Zebrafish: A resourceful vertebrate model to investigate skeletal disorders. *Front Endocrinol* (2020) 11:489. doi: 10.3389/fendo.2020.00489
- Valenti MT, Marchetto G, Mottes M, Carbonare LD. Zebrafish: A suitable tool for the study of cell signaling in bone. *Cells* (2020) 9(8):1911. doi: 10.3390/cells9081911
- Luderman LN, Unlu G, Knapik EW. Zebrafish developmental models of skeletal diseases. *Zebrafish at Interface Dev Dis Res* (2017) 124:81–124. doi: 10.1016/bs.ctdb.2016.11.004
- Mari-Beffa M, Mesa-Roman ABB, Duran I. Zebrafish models for human skeletal disorders. *Front Genet* (2021) 12:675331. doi: 10.3389/fgene.2021.675331
- Lleras-Forero L, Winkler C, Schulte-Merker S. Zebrafish and medaka as models for biomedical research of bone diseases. *Dev Biol* (2020) 457(2):191–205. doi: 10.1016/j.ydbio.2019.07.009
- Carnovali M, Banfi G, Mariotti M. Zebrafish models of human skeletal disorders: Embryo and adult swimming together. *BioMed Res Int* (2019) 2019:1253710. doi: 10.1155/2019/1253710
- Dietrich K, Fiedler IAK, Kurzyukova A, Lopez-Delgado AC, McGowan LM, Geurtzen K, et al. Skeletal biology and disease modeling in zebrafish. *J Bone Mineral Res* (2021) 36(3):436–58. doi: 10.1002/jbmr.4256
- Witten PE, Huysseune A. A comparative view on mechanisms and functions of skeletal remodelling in teleost fish, with special emphasis on osteoclasts and their function. *Biol Rev Camb Philos Soc* (2009) 84(2):315–46. doi: 10.1111/j.1469-185X.2009.00077.x
- Hall BK. *Bones and cartilage*. 2nd ed. Amsterdam, Netherlands: Academic Press (2015). p. 920.
- DeSesso JM, Scialli AR. Bone development in laboratory mammals used in developmental toxicity studies. *Birth Defects Res* (2018) 110(15):1157–87. doi: 10.1002/bdr2.1350
- Cubbage CC, Mabee PM. Development of the cranium and paired fins in the zebrafish *Danio rerio* (Ostariophysi, cyprinidae). *J Morphology* (1996) 229(2):121–60. doi: 10.1002/(sici)1097-4687(199608)229:2<121::aid-jmor1>3.0.co;2-4
- Kawasaki K, Richtsmeier JT. Association of the chondrocranium and dermatocranium in early skull formation. In: Percival C, Richtsmeier J, editors. *Building bones: Early bone development informing anthropological inquiry*. Cambridge, England: Cambridge University Press (2017). p. 52–78.
- de Beer GR. *The development of the vertebrate skull*. London: Oxford University Press (1937). p. 552.

Conflict of interest

The authors declare that the research was conducted in the absence of any commercial or financial relationships that could be construed as a potential conflict of interest.

Publisher's note

All claims expressed in this article are solely those of the authors and do not necessarily represent those of their affiliated organizations, or those of the publisher, the editors and the reviewers. Any product that may be evaluated in this article, or claim that may be made by its manufacturer, is not guaranteed or endorsed by the publisher.

- Netter FH. *Atlas of human anatomy*. 7th ed. Amsterdam, Netherlands: Elsevier (2018). p. 640.
- Fleming A, Kishida MG, Kimmel CB, Keynes RJ. Building the backbone: The development and evolution of vertebral patterning. *Development* (2015) 142(10):1733–44. doi: 10.1242/dev.118950
- Peskin B, Henke K, Cumplido N, Treaster S, Harris MP, Bagnat M, et al. Notochordal signals establish phylogenetic identity of the teleost spine. *Curr Biol* (2020) 30(14):2805–14. doi: 10.1016/j.cub.2020.05.037
- Bird NC, Mabee PM. Developmental morphology of the axial skeleton of the zebrafish, *Danio rerio* (Ostariophysi : Cyprinidae). *Dev Dynamics* (2003) 228(3):337–57. doi: 10.1002/dvdy.10387
- Bird NC, Hernandez LP. Building an evolutionary innovation: Differential growth by growth plates in the modified vertebral elements of the zebrafish weberian apparatus. *Zoology* (2009) 112(2):97–112. doi: 10.1016/j.zool.2008.05.003
- Grandel H, Schulte-Merker S. The development of the paired fins in the zebrafish (*Danio rerio*). *Mech Dev* (1998) 79(1-2):99–120. doi: 10.1016/s0925-4773(98)00176-2
- Hawkins MB, Henke K, Harris MP. Latent developmental potential to form limb-like skeletal structures in zebrafish. *Cell* (2021) 184(4):899–911. doi: 10.1016/j.cell.2021.01.003
- Giovannone D, Paul S, Schindler S, Arata C, Farmer DT, Patel P, et al. Programmed conversion of hypertrophic chondrocytes into osteoblasts and marrow adipocytes within zebrafish bones. *Elife* (2019) 8:e42736. doi: 10.7554/eLife.42736
- Wilsman NJ, Farnum CE, Leiferman EM, Fry M, Barreto C. Differential growth by growth plates as a function of multiple parameters of chondrocytic kinetics. *J Orthopaedic Res* (1996) 14(6):927–36. doi: 10.1002/jor.1100140613
- LeClair EE, Mui SR, Huang A, Topczewska JM, Topczewski J. Craniofacial skeletal defects of adult zebrafish glypican 4 (Knypek) mutants. *Dev Dynamics* (2009) 238(10):2550–63. doi: 10.1002/dvdy.22086
- Heubel BP, Bredesen CA, Schilling TF, Le Pabic P. Endochondral growth zone pattern and activity in the zebrafish pharyngeal skeleton. *Dev Dynamics* (2021) 250(1):74–87. doi: 10.1002/dvdy.241
- Wei X, Hu M, Mishina Y, Liu F. Developmental regulation of the growth plate and cranial synchondrosis. *J Dental Res* (2016) 95(11):1221–9. doi: 10.1177/0022034516651823
- Haines RW. Epiphyseal growth in the branchial skeleton of fishes. *Q J Microscopical Sci* (1934) 77:77–97. doi: 10.1242/jcs.s2-77.305.77
- Haines RW. The evolution of epiphyses and of endochondral bone. *Biol Rev* (1942) 17:267–92. doi: 10.1111/j.1469-185X.1942.tb00440.x
- Xie M, Gol'din P, Herdina AN, Estefa J, Medvedeva EV, Li L, et al. Secondary ossification center induces and protects growth plate structure. *Elife* (2020) 9:e55212. doi: 10.7554/eLife.55212
- Witten PE, Hansen A, Hall BK. Features of mono- and multinucleated bone resorbing cells of the zebrafish *Danio rerio* and their contribution to skeletal

development, remodeling, and growth. *J Morphology* (2001) 250(3):197–207. doi: 10.1002/jmor.1065.abs

33. Weigele J, Franz-Odenaal TA. Functional bone histology of zebrafish reveals two types of endochondral ossification, different types of osteoblast clusters and a new bone type. *J Anat* (2016) 229(1):92–103. doi: 10.1111/joa.12480
34. White A, Wallis G. Endochondral ossification: A delicate balance between growth and mineralisation. *Curr Biol* (2001) 11(15):R589–R91. doi: 10.1016/s0960-9822(01)00359-1
35. Maisey JG. Phylogeny of early vertebrate skeletal induction and ossification patterns. *Evolutionary Biol* (1988) 22:1–36. doi: 10.1007/978-1-4613-0931-4_1
36. Haines RW. The posterior end of meckel's cartilage and related ossifications in bony fishes. *J Cell Sci* (1937) s2-80(317):1–38. doi: 10.1242/jcs.s2-80.317.1
37. Huysseune A. *Skeletal system*. London: Academic Press (2000) p. 307–17.
38. Amatruda JF, Zon LI. Dissecting hematopoiesis and disease using the zebrafish. *Dev Biol* (1999) 216(1):1–15. doi: 10.1006/dbio.1999.9462
39. Rousseau F, Bonaventure J, Legeaimallet L, Pelet A, Rozet JM, Maroteaux P, et al. Mutations in the gene encoding fibroblast growth-factor receptor-3 in achondroplasia. *Nature* (1994) 371(6494):252–4. doi: 10.1038/371252a0
40. Shiang R, Thompson LM, Zhu YZ, Church DM, Fielder TJ, Bocian M, et al. Mutations in the transmembrane domain of Fgfr3 cause the most common genetic form of dwarfism, achondroplasia. *Cell* (1994) 78(2):335–42. doi: 10.1016/0092-8674(94)90302-6
41. Stanescu R, Stanescu V, Maroteaux P. Homozygous achondroplasia - morphological and biochemical study of cartilage. *Am J Med Genet* (1990) 37(3):412–21. doi: 10.1002/ajmg.1320370323
42. Blakemore L, Schwend R, Akbarnia BA, Dumas M, Schmidt J. Growth patterns of the neurocentral synchondrosis (Ncs) in immature cadaveric vertebra. *J Pediatr Orthopaedics* (2018) 38(3):181–4. doi: 10.1097/bpo.0000000000000781
43. Graham A. Deconstructing the pharyngeal metamere. *J Exp Zoology Part B-Molecular Dev Evol* (2008) 310B(4):336–44. doi: 10.1002/jez.b.21182
44. Kimmel CB, Miller CT, Keynes RJ. Neural crest patterning and the evolution of the jaw. *J Anat* (2001) 199:105–20. doi: 10.1046/j.1469-7580.2001.19910105.x
45. Eames BF, Yan YL, Swartz ME, Levic DS, Knapik EW, Postlethwait JH, et al. Mutations in fam20b and xylt1 reveal that cartilage matrix controls timing of endochondral ossification by inhibiting chondrocyte maturation. *PLoS Genet* (2011) 7(8):e1002246. doi: 10.1371/journal.pgen.1002246
46. Hoyle DJ, Dranow DB, Schilling TF. Pthlh and mechanical force control early patterning of growth zones in the zebrafish craniofacial skeleton. *Development* (2022) 149(2):dev199826. doi: 10.1242/dev.199826
47. Kampen WU, Claassen H, Kirsch T. Mineralization and osteogenesis in the human first rib cartilage. *Ann Anatomy-Anatomischer Anzeiger* (1995) 177(2):171–7. doi: 10.1016/s0940-9602(11)80069-5
48. Byers S, Moore AJ, Byard RW, Fazzalari NL. Quantitative histomorphometric analysis of the human growth plate from birth to adolescence. *Bone* (2000) 27(4):495–501. doi: 10.1016/s8756-3282(00)00357-4
49. Cumplido N, Allende ML, Arratia G. From devo to evo: Patterning, fusion and evolution of the zebrafish terminal vertebra. *Front Zoology* (2020) 17(1). doi: 10.1186/s12983-020-00364-y
50. Keer S, Cohen K, May C, Hu YN, McMenamin S, Hernandez LP. Anatomical assessment of the adult skeleton of zebrafish reared under different thyroid hormone profiles. *Anatomical Record-Advances Integr Anat Evolutionary Biol* (2019) 302(10):1754–69. doi: 10.1002/ar.24139
51. Huysseune A. Skeletal system. In: Ostrandter GK, editor. *The laboratory fish*. London: Academic Press (2000). p. 307–17.
52. Hall BK, Miyake T. All for one and one for all: Condensations and the initiation of skeletal development. *Bioessays* (2000) 22(2):138–47. doi: 10.1002/(sici)1521-1878(200002)22:2<138::aid-bies5>3.0.co;2-4
53. Bertmar G. On the ontogeny of the chondral skull in characidae with a discussion on the chondrocranial base and visceral chondrocranium in fishes. *Acta Zoologica* (1959) 40:203–364. doi: 10.1111/j.1463-6395.1959.tb00397.x
54. Schilling TF, Kimmel CB. Musculoskeletal patterning in the pharyngeal segments of the zebrafish embryo. *Development* (1997) 124(15):2945–60. doi: 10.1242/dev.124.15.2945
55. Le Pabic P, Stellwag EJ, Scemama J-L. Embryonic development and skeletogenesis of the pharyngeal jaw apparatus in the cichlid Nile tilapia (*Oreochromis niloticus*). *Anatomical Record-Advances Integr Anat Evolutionary Biol* (2009) 292(11):1780–800. doi: 10.1002/ar.20960
56. Dewit J, Witten PE, Huysseune A. The mechanism of cartilage subdivision in the reorganization of the zebrafish pectoral fin endoskeleton. *J Exp Zoology Part B-Molecular Dev Evol* (2011) 316B(8):584–97. doi: 10.1002/jez.b.21433
57. Kimmel CB, Miller CT, Kruze G, Ullmann B, BreMiller RA, Larison KD, et al. The shaping of pharyngeal cartilages during early development of the zebrafish. *Dev Biol* (1998) 203(2):245–63. doi: 10.1006/dbio.1998.9016
58. Le Pabic P, Ng C, Schilling TF. Fat-dachous signaling coordinates cartilage differentiation and polarity during craniofacial development. *PLoS Genet* (2014) 10(10):e1004726. doi: 10.1371/journal.pgen.1004726
59. Huysseune A, Sire JY. Development of cartilage and bone tissues of the anterior part of the mandible in cichlid fish - a light and tem study. *Anatomical Rec* (1992) 233(3):357–75. doi: 10.1002/ar.1092330304
60. Topczewski J, Sepich DS, Myers DC, Walker C, Amores A, Lele Z, et al. The zebrafish glypican knypek controls cell polarity during gastrulation movements of convergent extension. *Dev Cell* (2001) 1(2):251–64. doi: 10.1016/s1534-5807(01)00005-3
61. Gao B, Song H, Bishop K, Elliot G, Garrett L, English MA, et al. Wnt signaling gradients establish planar cell polarity by inducing Vangl2 phosphorylation through Ror2. *Dev Cell* (2011) 20(2):163–76. doi: 10.1016/j.devcel.2011.01.001
62. Li YW, Dudley AT. Noncanonical frizzled signaling regulates cell polarity of growth plate chondrocytes. *Development* (2009) 136(7):1083–92. doi: 10.1242/dev.023820
63. Rochard L, Monica SD, Ling ITC, Kong Y, Roberson S, Harland R, et al. Roles of wnt pathway genes wls, Wnt9a, Wnt5b, frzb and Gpc4 in regulating convergent-extension during zebrafish palate morphogenesis. *Development* (2016) 143(14):2541–7. doi: 10.1242/dev.137000
64. Kamel G, Hoyos T, Rochard L, Dougherty M, Kong Y, Tse W, et al. Requirement for frzb and Fzd7a in cranial neural crest convergence and extension mechanisms during zebrafish palate and jaw morphogenesis. *Dev Biol* (2013) 381(2):423–33. doi: 10.1016/j.ydbio.2013.06.012
65. Li YW, Lie A, Junge J, Bronner M. Planar cell polarity signaling coordinates oriented cell division and cell rearrangement in clonally expanding growth plate cartilage. *Elife* (2017) 6:e23279. doi: 10.7554/eLife.23279
66. Sisson BE, Dale RM, Mui SR, Topczewska JM, Topczewski J. A role of Glypican4 and Wnt5b in chondrocyte stacking underlying craniofacial cartilage morphogenesis. *Mech Dev* (2015) 138:279–90. doi: 10.1016/j.mod.2015.10.001
67. Schwabe GC, Tinschert S, Buschow C, Meinecke P, Wolff G, Gillesen-Kaesbach G, et al. Distinct mutations in the receptor tyrosine kinase gene Ror2 cause brachydactyly type b. *Am J Hum Genet* (2000) 67(4):822–31. doi: 10.1086/303084
68. Oldridge M, Fortuna AM, Maringa M, Propping P, Mansour S, Pollitt C, et al. Dominant mutations in Ror2, encoding an orphan receptor tyrosine kinase, cause brachydactyly type b. *Nat Genet* (2000) 24(3):275–8. doi: 10.1038/73495
69. van Bokhoven H, Celli J, Kayserili H, van Beusekom E, Balci S, Brussel W, et al. Mutation of the gene encoding the Ror2 tyrosine kinase causes autosomal recessive robinow syndrome. *Nat Genet* (2000) 25(4):423–6. doi: 10.1038/78113
70. Afzal AR, Rajab A, Fenske CD, Oldridge M, Elanko N, Ternes-Pereira E, et al. Recessive robinow syndrome, allelic to dominant brachydactyly type b, is caused by mutation of Ror2. *Nat Genet* (2000) 25(4):419–22. doi: 10.1038/78107
71. White JJ, Mazzeu JF, Coban-Akdemir Z, Bayram Y, Bahrambeigi V, Hoischen A, et al. Wnt signaling perturbations underlie the genetic heterogeneity of robinow syndrome. *Am J Hum Genet* (2018) 102(1):27–43. doi: 10.1016/j.ajhg.2017.10.002
72. Lima AR, Ferreira BM, Zhang C, Jolly A, Du H, White JJ, et al. Phenotypic and mutational spectrum of Ror2-related robinow syndrome. *Hum Mutat* (2022) 43:900–18. doi: 10.1002/humu.24375
73. Person AD, Beiraghi S, Sieben CM, Hermanson S, Neumann AN, Robu ME, et al. Wnt5a mutations in patients with autosomal dominant robinow syndrome. *Dev Dyn* (2010) 239(1):327–37. doi: 10.1002/dvdy.22156
74. Waterson J, Stockley TL, Segal S, Golabi M. Novel duplication in glypican-4 as an apparent cause of Simpson-Golabi-Behmel syndrome. *Am J Med Genet A* (2010) 152A(12):3179–81. doi: 10.1002/ajmg.a.33450
75. Amor DJ, Stephenson SEM, Mustapha M, Mensah MA, Ockeloen CW, Lee WS, et al. Pathogenic variants in Gpc4 cause keipert syndrome. *Am J Hum Genet* (2019) 104(5):914–24. doi: 10.1016/j.ajhg.2019.02.026
76. Cappello S, Gray MJ, Badouel C, Lange S, Einsiedler M, Srour M, et al. Mutations in genes encoding the cadherin receptor-ligand pair Dchs1 and Fat4 disrupt cerebral cortical development. *Nat Genet* (2013) 45(11):1300–8. doi: 10.1038/ng.2765
77. Mansour S, Swinkels M, Terhal PA, Wilson LC, Rich P, Van Maldergem L, et al. Van maldergem syndrome: Further characterisation and evidence for neuronal migration abnormalities and autosomal recessive inheritance. *Eur J Hum Genet* (2012) 20(10):1024–31. doi: 10.1038/ejhg.2012.57
78. Yang L, Tsang KY, Tang HC, Chan D, Cheah KSE. Hypertrophic chondrocytes can become osteoblasts and osteocytes in endochondral bone formation. *Proc Natl Acad Sci United States America* (2014) 111(33):12097–102. doi: 10.1073/pnas.1302703111

79. Park J, Gebhardt M, Golovchenko S, Perez-Branguli F, Hattori T, Hartmann C, et al. Dual pathways to endochondral osteoblasts: A novel chondrocyte-derived osteoprogenitor cell identified in hypertrophic cartilage. *Biol Open* (2015) 4(5):608–21. doi: 10.1242/bio.201411031
80. Roach HI. New aspects of endochondral ossification in the chick: Chondrocyte apoptosis, bone formation by former chondrocytes, and acid phosphatase activity in the endochondral bone matrix. *J Bone Mineral Res* (1997) 12(5):795–805. doi: 10.1359/jbmr.1997.12.5.795
81. Roach HI. Transdifferentiation of hypertrophic chondrocytes into cells capable of producing a mineralized bone-matrix. *Bone Mineral* (1992) 19(1):1–20. doi: 10.1016/0169-6009(92)90840-a
82. Vortkamp A, Lee K, Lanske B, Segre GV, Kronenberg HM, Tabin CJ. Regulation of rate of cartilage differentiation by Indian hedgehog and pth-related protein. *Science* (1996) 273(5275):613–22. doi: 10.1126/science.273.5275.613
83. Chung UI, Lanske B, Lee KC, Li E, Kronenberg H. The parathyroid hormone parathyroid hormone-related peptide receptor coordinates endochondral bone development by directly controlling chondrocyte differentiation. *Proc Natl Acad Sci United States America* (1998) 95(22):13030–5. doi: 10.1073/pnas.95.22.13030
84. Chung UI, Schipani E, McMahon AP, Kronenberg HM. Indian Hedgehog couples chondrogenesis to osteogenesis in endochondral bone development. *J Clin Invest* (2001) 107(3):295–304. doi: 10.1172/jci11706
85. Clement A, Wiweger M, von der Hardt S, Rusch MA, Selleck SB, Chien CB, et al. Regulation of zebrafish skeletogenesis by *ext2/Dackel* and *papst1/Pinscher*. *PLoS Genet* (2008) 4(7):e1000136. doi: 10.1371/journal.pgen.1000136
86. St-Jacques B, Hammerschmidt M, McMahon AP. Indian Hedgehog signaling regulates proliferation and differentiation of chondrocytes and is essential for bone formation. *Genes Dev* (1999) 13(16):2072–86. doi: 10.1101/gad.13.16.2072
87. Retting KN, Song B, Yoon BS, Lyons KM. Bmp canonical smad signaling through Smad1 and Smad5 is required for endochondral bone formation. *Development* (2009) 136(7):1093–104. doi: 10.1242/dev.029926
88. Wang WG, Song B, Anbarchian T, Shirazyan A, Sadik JE, Lyons KM. Smad2 and Smad3 regulate chondrocyte proliferation and differentiation in the growth plate. *PLoS Genet* (2016) 12(10):e1006352. doi: 10.1371/journal.pgen.1006352
89. Colvin JS, Bohne BA, Harding GW, McEwen DG, Ornitz DM. Skeletal overgrowth and deafness in mice lacking fibroblast growth factor receptor 3. *Nat Genet* (1996) 12(4):390–7. doi: 10.1038/ng0496-390
90. Naski MC, Colvin JS, Coffin JD, Ornitz DM. Repression of hedgehog signaling and Bmp4 expression in growth plate cartilage by fibroblast growth factor receptor 3. *Development* (1998) 125(24):4977–88. doi: 10.1242/dev.125.24.4977
91. Long FX, Chung UI, Ohba S, McMahon J, Kronenberg HM, McMahon AP. *Ihh* signaling is directly required for the osteoblast lineage in the endochondral skeleton. *Development* (2004) 131(6):1309–18. doi: 10.1242/dev.01006
92. Felber K, Croucher P, Roehl HH. Hedgehog signalling is required for perichondral osteoblast differentiation in zebrafish. *Mech Dev* (2011) 128(1–2):141–52. doi: 10.1016/j.mod.2010.11.006
93. Cooper KL, Oh S, Sung Y, Dasari RR, Kirschner MW, Tabin CJ. Multiple phases of chondrocyte enlargement underlie differences in skeletal proportions. *Nature* (2013) 495(7441):375–8. doi: 10.1038/nature11940
94. Young B, Minugh-Purvis N, Shimo T, St-Jacques B, Iwamoto M, Enomoto-Iwamoto M, et al. Indian And sonic hedgehogs regulate synchondrosis growth plate and cranial base development and function. *Dev Biol* (2006) 299(1):272–82. doi: 10.1016/j.ydbio.2006.07.028
95. Nagayama M, Iwamoto M, Hargett A, Kamiya N, Tamamura Y, Young B, et al. Wnt/Beta-catenin signaling regulates cranial base development and growth. *J Dental Res* (2008) 87(3):244–9. doi: 10.1177/154405910808700309
96. Eames BF, Singer A, Smith GA, Wood ZA, Yan YL, He XJ, et al. Udp xylose synthase 1 is required for morphogenesis and histogenesis of the craniofacial skeleton. *Dev Biol* (2010) 341(2):400–15. doi: 10.1016/j.ydbio.2010.02.035
97. Farnum CE, Tinsley M, Hermanson JW. Forelimb versus hindlimb skeletal development in the big brown bat, *Eptesicus fuscus*: Functional divergence is reflected in chondrocytic performance in autopodial growth plates. *Cells Tissues Organs* (2008) 187(1):35–47. doi: 10.1159/000109962
98. Johnson S, Heubel B, Bredesen C, Schilling T, Le Pabic P. Cellular basis of differential endochondral growth in lake Malawi cichlids. *Dev Dynamics* (2022) 1–14. doi: 10.1002/dvdy.529
99. Huyssseune A, Verraes W, Desender K. Mechanisms of branchial cartilage growth in *Astatotilapia elegans* (Teleostei: Cichlidae). *J Anat* (1988) 158:13–30.
100. Borjesson AE, Lagerquist MK, Windahl SH, Ohlsson C. The role of estrogen receptor alpha in the regulation of bone and growth plate cartilage. *Cell Mol Life Sci* (2013) 70(21):4023–37. doi: 10.1007/s00018-013-1317-1
101. Ford E. Growth of the human cranial base. *Am J Orthodontics* (1958) 44:498–506. doi: 10.1016/0002-9416(58)90082-4
102. Scott JH. The cranial base. *Am J Phys Anthropol* (1958) 16:319–48. doi: 10.1002/ajpa.1330160305
103. Hayashi I. Morphological relationship between the cranial base and dentofacial complex obtained by reconstructive computer tomographic images. *Eur J Orthodontics* (2003) 25(4):385–91. doi: 10.1093/ejo/25.4.385
104. von Bertalanffy L. A quantitative theory of organic growth (Inquiries on growth laws. ii). *Hum Biol* (1938) 10:181–213. Available at: <https://www.jstor.org/stable/41447359>
105. Schilling TF. The morphology of larval and adult zebrafish. In: Nusslein-Volhard C, Dahm R, editors. *Zebrafish: A practical approach*. New York: Oxford University Press (2002).
106. Parichy DM, Elizondo MR, Mills MG, Gordon TN, Engeszer RE. Normal table of postembryonic zebrafish development: Staging by externally visible anatomy of the living fish. *Dev Dynamics* (2009) 238(12):2975–3015. doi: 10.1002/dvdy.22113
107. Brown DS, Eames BF. Emerging tools to study proteoglycan function during skeletal development. *Zebrafish: Cell Dev Biology Pt B: Dev Biol* (2016) 134:485–530. doi: 10.1016/bs.mcb.2016.03.001
108. Alvarez C, Tredwell S, De Vera M, Hayden M. The genotype-phenotype correlation of hereditary multiple exostoses. *Clin Genet* (2006) 70(2):122–30. doi: 10.1111/j.1399-0004.2006.00653.x
109. Francannet C, Cohen-Tanugi A, Le Merrer M, Munnich A, Bonaventure J, Legeai-Mallet L. Genotype-phenotype correlation in hereditary multiple exostoses. *J Med Genet* (2001) 38(7):430–4. doi: 10.1136/jmg.38.7.430
110. Xu L, Xia JH, Jiang HJ, Zhou JN, Li HJ, Wang DP, et al. Mutation analysis of hereditary multiple exostoses in the Chinese. *Hum Genet* (1999) 105(1–2):45–50. doi: 10.1007/s004390051062
111. Varshney GK, Pei WH, LaFave MC, Idol J, Xu LS, Gallardo V, et al. High-throughput gene targeting and phenotyping in zebrafish using Crispr/Cas9. *Genome Res* (2015) 25(7):1030–42. doi: 10.1101/gr.186379.114
112. Wu RS, Lam II, Clay H, Duong DN, Deo RC, Coughlin SR. A rapid method for directed gene knockout for screening in G0 zebrafish. *Dev Cell* (2018) 46(1):112–25. doi: 10.1016/j.devcel.2018.06.003
113. Hammond C, Moro E. Using transgenic reporters to visualize bone and cartilage signaling during development in vivo. *Front Endocrinol* (2012) 3:91. doi: 10.3389/fendo.2012.00091
114. Kimmel CB, DeLaurier A, Ullmann B, Dowd J, McFadden M. Modes of developmental outgrowth and shaping of a craniofacial bone in zebrafish. *PLoS One* (2010) 5(3):12. doi: 10.1371/journal.pone.0009475
115. Curado S, Stainier D, Anderson RM. Nitroreductase-mediated Cell/Tissue ablation in zebrafish: A spatially and temporally controlled ablation method with applications in developmental and regeneration studies. *Nat Protoc* (2008) 3(6):948–54. doi: 10.1038/nprot.2008.58
116. Kawakami K, Shima A. Identification of the Tol2 transposase of the medaka fish *Oryzias latipes* that catalyzes excision of a nonautonomous Tol2 element in zebrafish *Danio rerio*. *Gene* (1999) 240(1):239–44. doi: 10.1016/s0378-1119(99)00444-8
117. Kwan KM, Fujimoto E, Grabher C, Mangum BD, Hardy ME, Campbell DS, et al. The Tol2kit: A multisite gateway-based construction kit for Tol2 transposon transgenesis constructs. *Dev Dyn* (2007) 236(11):3088–99. doi: 10.1002/dvdy.21343
118. Farrell JA, Wang YQ, Riesenfeld SJ, Shekhar K, Regev A, Schier AF. Single-cell reconstruction of developmental trajectories during zebrafish embryogenesis. *Science* (2018) 360(6392):979–85. doi: 10.1126/science.aar3131
119. Raj B, Wagner DE, McKenna A, Pandey S, Klein AM, Shendure J, et al. Simultaneous single-cell profiling of lineages and cell types in the vertebrate brain. *Nat Biotechnol* (2018) 36(5):442–50. doi: 10.1038/nbt.4103
120. Lencer E, Prekeris R, Artinger KB. Single-cell RNA analysis identifies premigratory neural crest cells expressing markers of differentiated derivatives. *Elife* (2021) 10:e66078. doi: 10.7554/eLife.66078
121. Fabian P, Tseng KC, Thiruppathy M, Arata C, Chen HJ, Smeeton J, et al. Lifelong single-cell profiling of cranial neural crest diversification in zebrafish. *Nat Commun* (2022) 13(13). doi: 10.1038/s41467-021-27594-w
122. Wagner DE, Weinreb C, Collins ZM, Briggs JA, Megason SG, Klein AM. Single-cell mapping of gene expression landscapes and lineage in the zebrafish embryo. *Science* (2018) 360(6392):981–7. doi: 10.1126/science.aar4362